Article

Journal of
Nanoscience and Nanotechnology
Vol. 15, 7645–7651, 2015
www.aspbs.com/jnn

Enhancement of Characteristics of a Touch Sensor by Controlling the Multi-Layer Architecture of a Low-Cost Metal Mesh Pattern

Seung-Hoon Kwak[1, 2], Min-Gi Kwak[1], Byeong-Kwon Ju[2, *], and Sung-Jei Hong[1, *]

[1] *Display Components and Materials Research Center, Korea Electronics Technology Institute, Seongnam, Gyeonggi-do 463-816, Korea*
[2] *School of Electrical Engineering, Korea University, Seoul 136-713, Korea*

In this study, the characteristics of a metal mesh touch sensor were enhanced by optimizing the multi-layer architecture of the metal mesh pattern. Low-cost metal such as an aluminum (Al) layer was mainly applied to the architectures for practical applications in touch screen panel (TSP) industries. As well, molybdenum (Mo) was added to the architectures in order to minimize the drawbacks of Al. Three types of Mo/Al, Al/Mo and Mo/Al/Mo layers were fabricated by DC sputtering. The thickness of the Al and Mo layer was optimized at 150 and 30 nm, respectively. Low sheet resistance below 0.27 Ω/□ was achieved with good adhesion on a glass substrate. Especially, in the case of architectures in which the Al layer was covered with an Mo layer, thermal stability and corrosion resistance was enhanced. The change in resistance of the Mo/Al/Mo architecture was less than 0.056 even after heat-treatment at 260 °C. By using the optimized layer architecture, the mesh pattern with a 4 μm line width showed good optical transmittance (86.7%) and reflectivity (13.1%) at 550 nm, respectively. Also, a touch sensor fabricated by using the Mo/Al/Mo mesh pattern operated well indicating that the mesh pattern is feasible in a TSP application.

Keywords: Touch Screen Panel, Touch Sensor, Metal Mesh, Low Cost Multi-Layer, Resistance, Transmittance, Reflectivity.

1. INTRODUCTION

Recently, touch screen panels (TSPs) have been commercialized in applications such as smart phones, smart pads, tablet PCs, and other displays, etc.[1] Moreover, the demand for commercialization of TSPs is continuously increasing in home, industry, and mobile applications.[2] In order to be practical in a wide range of applications, a touch panel must be rugged, fast, precise, impervious to common chemicals, and easy to integrate into common electronic devices.[3] TSPs are consistent of touch sensors on glass or polymeric films, and the touch sensors determine the function of the TSPs. Among the several types of touch sensors, capacitive-type touch sensors are known to be practical.[3]

Most capacitive touch sensors contain an indium-tin-oxide (ITO) layer as sensing materials that possess the unique properties of high optical transparency and electrical conductivity.[4] ITO has been widely used as a transparent conductor material consisting of indium oxide and tin oxide in a ratio of 9 to 1. However, due to the high cost of indium at its source, means of reducing indium usage have been widely investigated, including metal films.[5] Metal films such as silver (Ag) and copper (Cu) are considered desirable owing to their higher electrical conductivity and superior durability, and attract much attention for medium and large TSPs.[6] To ensure high optical transmittance, metal films have to be patterned with a width of less than 5 μm.[5] In the case of printing method, however, it is difficult to fabricate metal mesh having a grid width of less than 10 μm.[5] Moreover, from a commercial point of view, the cost of the metal films have to be as low as possible.

In this study, low cost aluminum (Al) mesh was fabricated on glass substrate by the DC sputtering method to investigate the characteristics of the touch sensing layer. In addition, to enhance durability, a molybdenum (Mo)

*Authors to whom correspondence should be addressed.

layer was added to the Al mesh layer. By controlling the multi-layer architecture of the metal mesh pattern, low cost metal mesh type touch sensors were attempted to enhance the characteristics.

2. EXPERIMENTAL DETAILS

As depicted in Figure 1, three types of metal mesh architectures were prepared. Type 1 consists of a Mo/Al double layer architecture on which Mo was deposited over the bottom Al layer. Type 2 has an Al/Mo double layer architecture, and Al was deposited over the bottom Mo layer. Type 3 has a triple layer architecture of Mo/Al/Mo. All the samples were fabricated on a glass substrate with a size of 10×10 cm and 700 μm thickness. As well, even though not depicted in the figure, all the samples contain an anti-reflection layer. Al and Mo were deposited on the glass substrate by DC sputtering with various thicknesses. For sputtering, a 6″-sized Al and Mo sputtering target with a purity of 99.999% was used, respectively. The optimized sputtering conditions of Al and Mo are summarized in Table I. The sputtering rate of the Al and Mo layer was 12 nm and 6 nm, respectively. To observe the thermal stability of the architectures, the samples were heated at a temperature ranging from 200, 220, 240, and 260 °C for 1 hour using a box-type furnace, respectively. As well, a corrosion test was done by dipping the samples in a Tetramethyl ammonium hydroxide (TMAH) solution, which is used as a developer for the patterning of metal mesh at room temperature. The architecture was optimized with thermal and corrosion tests, and the metal mesh pattern of the optimized architecture was fabricated by using photo-lithography followed by etching of the multi-metal layer. Line with of the patterns were designed as 4 μm and 5 μm and fabricated for comparison. The detailed fabrication process is shown in Figure 2.

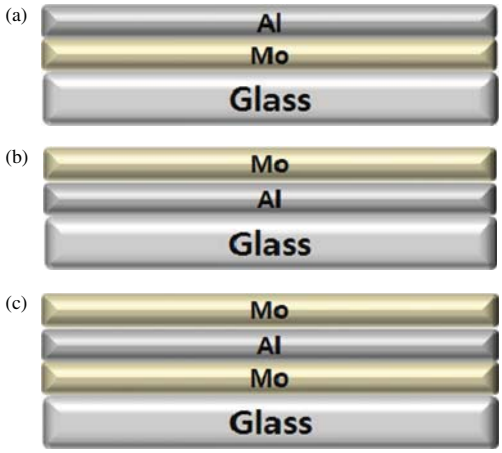

Figure 1. Schematic diagrams of three different types of metal layers. (a) Mo/Al double layer (type 1), (b) Al/Mo double layer (type 2), and (c) Mo/Al/Mo triple layer (type 3) architectures.

Table I. Sputtering conditions of Al and Mo layers.

Layers	Al	Mo
Base pressure	4.5×10^{-6} Torr	4.0×10^{-6} Torr
Insert gas	Ar (60 SCCM)	Ar (60 SCCM)
Working pressure	4.5 mTorr	4.5 mTorr
Power	300 W	150 W
Temperature	Room temperature	Room temperature

The optical and electrical properties of the samples were investigated with a UV-VIS spectrophotometer (JASCO, V-560) and a 4-point probe electrical measurement system (Mitsubishi Chemical Analytech, MCP-T610), respectively. As well, an adhesion test was performed according to the ASTM standard D 3359–97,[7] that is, the surface of the deposited metal layer was scratched with 10×10 cut-lines, and a peel-off test with tape was done followed by observation of the pelt-off behavior.

Finally, a touch sensor was fabricated using a mesh pattern with the optimized architecture, and a flexible printed circuit board (FPCB) was attached to the pattern using anisotropic conductive film (ACF). Then, the FPCB was connected to the computer including the IC controller and program to operate the TSP. The operation of the touch sensor was attempted to determine whether the optimized layer architecture is feasible with TSP.

3. RESULTS AND DISCUSSION

The surface microstructures of the three types of architectures are shown in Figures 3(a)–(c). Particles of the surface are very fine and uniform, which is attributed to the

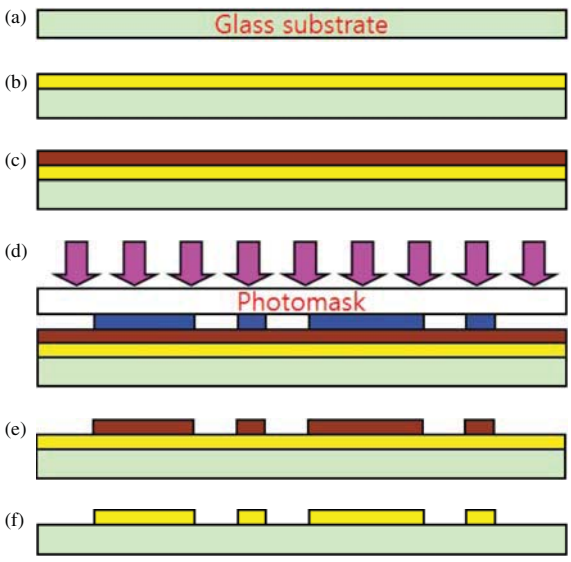

Figure 2. Fabrication process of metal mesh pattern. (a) preparation of glass substrate (b) deposition of Al and Mo layers (c) coating of photoresist (d) exposure (e) developing of photoresist (f) etching of metal layers followed by removal of residual photoresist.

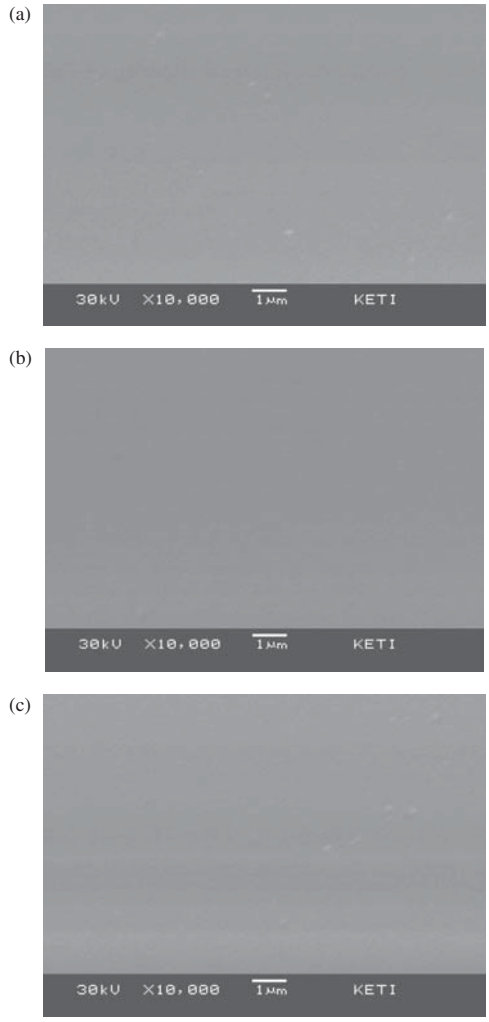

Figure 3. Surface microstructures of sample (a) type 1 (Mo/Al) (b) type 2 (Al/Mo) and (c) type 3 (Mo/Al/Mo) layer architectures.

uniform sputtering of Mo and Al in the vacuum chamber. Then, the adhesions of the architectures were investigated. In the case of type 2 (Al/Mo), the layer was partially pelt off after testing as shown in Figure 4(b), whereas in the case of type 1 (Mo/Al) and 3 (Mo/Al/Mo), the layers were rarely pelt off after testing as shown in Figures 4(a) and (c). This performance is owing to the superior adhesion of the Mo thin film. It is known that the Mo layer is widely used as a bottom layer because of its good adhesion,[8] and exhibits superior adhesion by sputtering under optimal conditions.[9] Likewise, it is guessed that the Mo layer deposited on the glass substrate under optimal conditions exhibited good adhesion.

Prior to investigating the sheet resistances of the samples, Al and Mo layers with different thicknesses were deposited and measured to investigate the sheet resistance of each Al and Mo layer. In Figure 5(a), the sheet

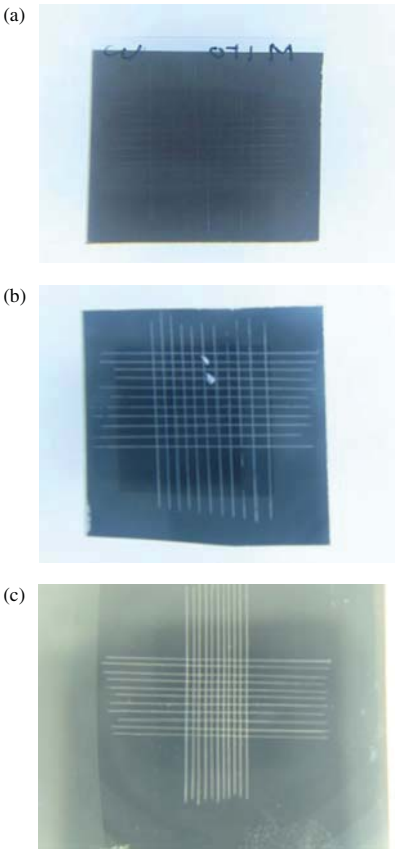

Figure 4. Adhesion of smaple (a) type 1 (Mo/Al) (b) type 2 (Al/Mo) and (c) type 3 (Mo/Al/Mo) layer architectures.

resistances of the Al layers with thicknesses of 130, 140, 150, 160, 170 and 180 nm were 0.43, 0.33, 0.29, 0.27, 0.24 and 0.23 Ω/□, respectively. Also, as shown in Figure 5(b), the sheet resistances of the Mo layer with thicknesses of 5, 10, 15, 20, 25 and 30 nm were 127, 65, 35, 30, 15 and 15 Ω/□, respectively. Mo layers were deposited with thicknesses lower than those of Al considering the cost-savings. As a result, the sheet resistance decreased as the thickness increased. This reaction is owing to the thickness dependence of the metallic layer.[10] The sheet resistance is determined using the simple relation:

$$R_s = \rho/t \tag{1}$$

where R_s, ρ, and t are sheet resistance, resistivity, and thickness. From the relation (1), assuming that the resistivity is constant, the sheet resistance is inproportional to the thickness. As the thickness increases, the sheet resistance decreases. In addition, besides the influence of thickness, the sheet resistance of the Al layer is lower than that of the Mo layer, which is owing to the difference in resistivity between the two materials, i.e., the resistivity of Al and Mo is 2.820×10^{-2} and 5.225×10^{-2} $\mu\Omega \cdot$cm, respectively.

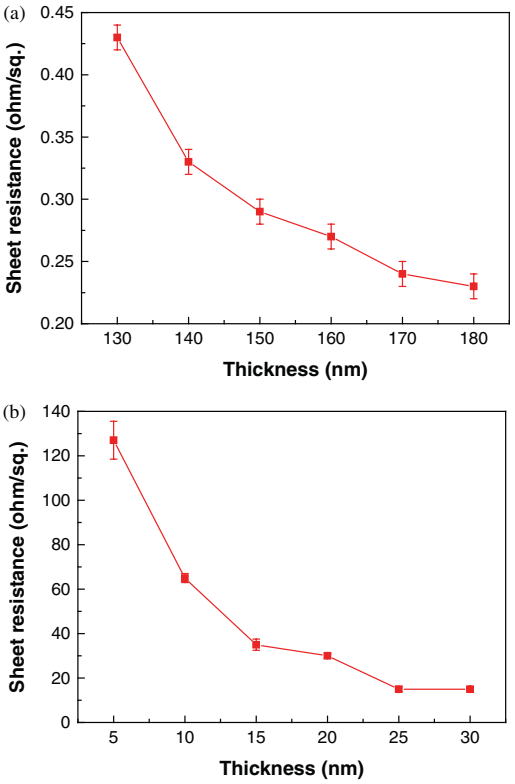

Figure 5. Sheet resistance of (a) Al and (b) Mo layers with different thickness.

Because the resistivity of Al is lower than that of Mo, the sheet resistance of Al is lower than that of Mo even at the same thickness.

However, it is known that corrosion resistance of Mo is higher than that of Al,[11] i.e., corrosion attack of the surface of Al is inhibited by the Mo layer coated on its surface. Thus, to optimize the layer architecture, three types were fabricated as mentioned. Considering the sheet resistance obtained from Figure 5, the thicknesses of Al and Mo were fixed at 150 and 30 nm, respectively. As a result, the sheet resistances of type 1, 2 and 3 were measured as 0.272, 0.261 and 0.252 Ω/□, respectively.

Then, the thermal stability of the samples was investigated. The most commonly used method for prediction due to thermal failure can be described by the following equation:

$$t_e = t_a \times 2.5 \cdot \exp\left(\frac{T_a - T_c}{10}\right) \quad (2)$$

where t_e is the lifetime under normal temperature T_c and t_a is the life under the accelerated condition T_a. This equation is widely used in electronics to extrapolate cumulative failure.[12] In fact, according to the JEDEC standard,[13] a high-temperature storage test is done by maintaining samples for 500 hours at 125 °C. In this study, 1 hour at more

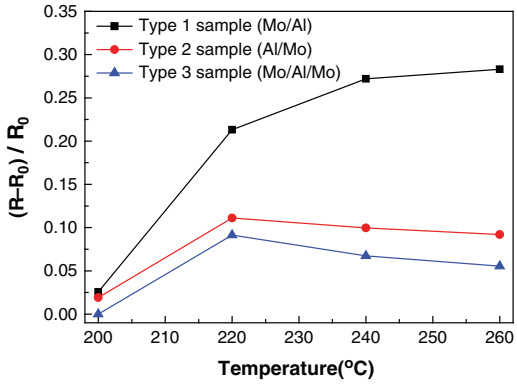

Figure 6. Change in sheet resistance according to storage temperature.

than 200 °C is equivalent to more than 2.5×10^7 hours at 125 °C. The change in resistance is expressed as $(R - R_0)/R_0$, where R_0 is the initial resistance and R is the measured resistance after aging. As shown in Figure 6, $(R - R_0)/R_0$ of type 1 after aging at 200, 220, 240 and 260 °C for 1 hour was 0.026, 0.2132, 0.2721 and 0.2831, respectively. $(R - R_0)/R_0$ increases steeply from 200 to 220 °C and, above 220 °C, it steadily increases as temperature is raised. A similar tendency of behavior was observed from type 2. However, the value of $(R - R_0)/R_0$ is almost a half of those of type 1. That is, $(R - R_0)/R_0$ after aging at 200, 220, 240 and 260 °C for 1 hour was 0.019, 0.1111, 0.0996 and 0.0919. Moreover, $(R - R_0)/R_0$ of type 3 after aging at 200, 220, 240 and 260 °C for 1 hour was 0.000, 0.0913, 0.0675 and 0.0556, respectively. Type 3 is more stable than type 2 in spite of the rising temperature. The stable behavior of type 3 is related to the superior oxidation resistance of the Mo layer. It has been reported that inward-diffusion of oxygen is suppressed by Mo leading to suppression of formation and the growth of oxide.[14] From the architectures of type 2 and 3 that Mo layer is on top of the Al layer, it is guessed that the Mo layer

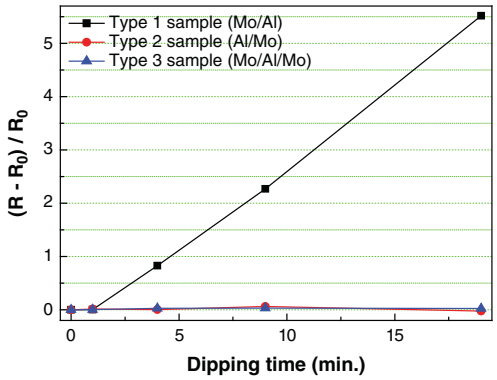

Figure 7. Change in sheet resistance according to sample of dipping time in TMAH developer at room temperature.

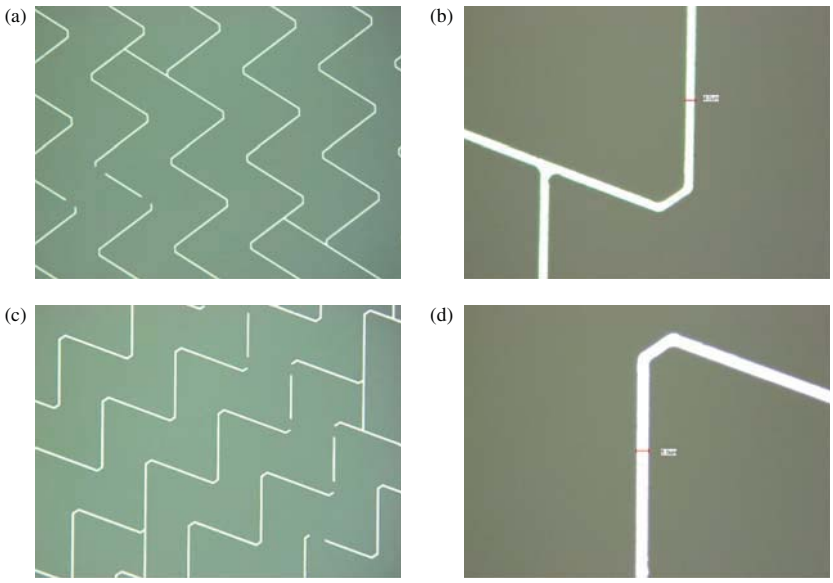

Figure 8. Mo/Al/Mo mesh patterns with line width of (a) and (b) 4 μm, and (c) and (d) 5 μm.

blocks out the inward-diffusion of oxygen to the Al layer, i.e., suppression of oxidation of the Al layer leading to a decrease change in resistance.

From the thermal test, it was demonstrated that the Mo layer on top of the Al layer increases the life-time of the architectures. Also, the corrosion resistance of the architectures is important. Especially, the TMAH developer used in this study is known to attack base metals such as Al. If the metallic layer is attacked by the corrosive reagent, sheet resistance is predicted to increase. Thus, we investigated the corrosion behavior of the samples by dipping then in the TMAH solution for several minutes. In Figure 7, $(R-R_0)/R_0$ of the type 1 sample was 0.0041, 0.8293, 2.2683 and 5.5163 after dipping for 1, 4, 9 and 19 min at room temperature, respectively. A considerable increase in sheet resistance was observed. In type 2 and 3, however, increases of sheet resistance were neglible. After dipping for 1, 4, 9 and 19 min. at room temperature, $(R-R_0)/R_0$ of the type 2 sample was 0.0122, 0.0041, 0.0610 and 0.0244 in absolute units. As well, under the same conditions, $(R-R_0)/R_0$ of type 3 sample was 0.0040, 0.0278, 0.0318 and 0.0238. Compared to type 1, the stability of type 2 and 3 were remarkably improved. Those phenomena are attributed to the increase of corrosion resistance by covering Al with Mo. It has been reported that the presence of Mo on Al highly affects the corrosion behavior because of the enhancement of the cathodic reaction when the electrolyte reaches Mo zones, and that effect increases the development of more occluded forms of corrosion.[15] This means that the corrosion of Mo is superior to that of Al. Thus, it is guessed that the corrosion resistance was enhanced by covering the Al layer with the Mo layer, and it led to the stable behavior of the sheet resistance even after being dipped in the corrosive reagent for a long time.

From the thermal and corrosion tests, it has been clarified that the architectures of the Mo layer on top of the

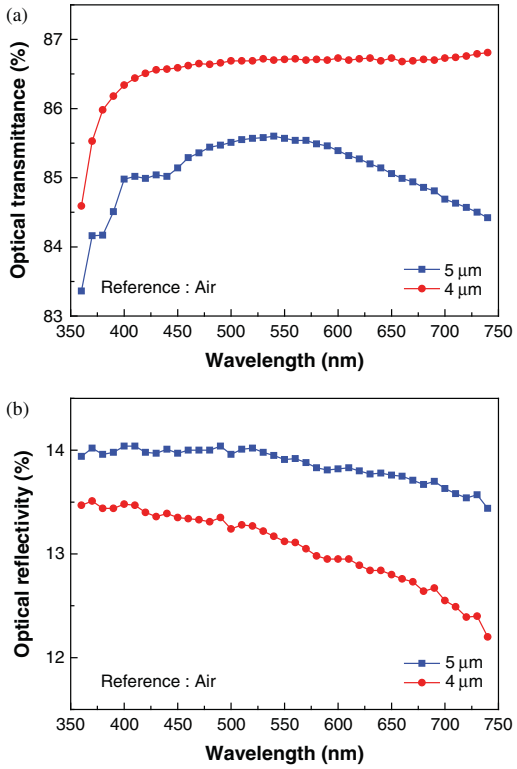

Figure 9. Optical properties of Mo/Al/Mo layer. (a) optical transmittance and (b) optical reflectivity.

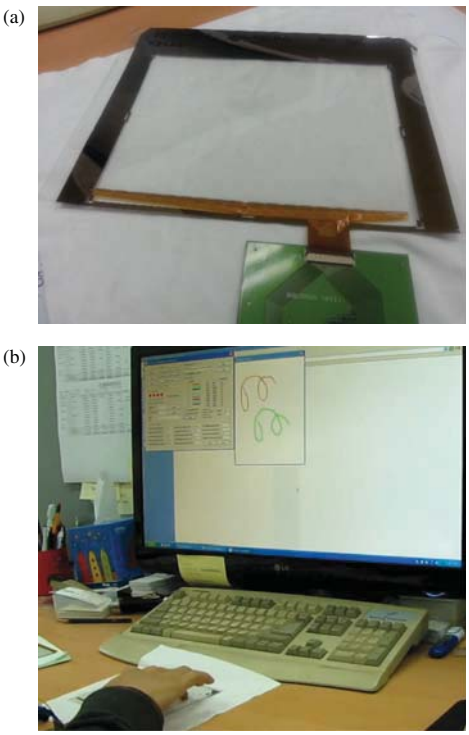

Figure 10. Touch screen panel fabricated with 4 μm line width Mo/Al/Mo mesh pattern (a) after fabrication (b) with operation.

Al layer enhance the characteristics. Especially, type 3 (Mo/Al/Mo) enhances the thermal stability and corrosion resistance. Therefore, using the type 3 mesh pattern, the touch sensors were fabricated with photo-lithography. Two types of line width, 4 and 5 μm, were designed and fabricated (as shown in Fig. 8). Then, the optical properties of the two samples were investigated. The transmittance of the metal mesh pattern was increased as the pattern width was decreased. As shown in Figure 9(a), at a wavelength of 550 nm, which is the central range of visible light, the optical transmittances of the samples with a width of 4 and 5 μm were 86.7 and 85.6%, respectively. As well, as shown in Figure 9(b), their optical reflectivities were 13.1 and 13.9% at 550 nm. From the results, it is known that the optical properties of the metal mesh patterns are affected by the width of the metal mesh pattern.

The transmittance and reflectivity are important optical properties used as TSP. As a light beam falls into a TSP, it reflects at the external and also internal surface, attenuates in the interior of the film, and the rest of it transmits through the substrate.[16] The ratio of the intensities of the reflected and attenuated light to that of the incident beam is termed as reflectance, R, and attenuation, A, respectively. The total amount of light emerging from the film is termed as total transmittance, T. According to the law of conservation of energy, they have a relationship as follows:[17]

$$T + R + A = 1 \tag{3}$$

In order to obtain high T, the R and A must be reduced. One of the solutions to reduce attenuation is to decrease the width of the mesh pattern. Thus, it is guessed that a mesh pattern with a 4 μm width exhibits superior optical properties to that with a 5 μm width.

Finally, the feasibility of the optimized mesh pattern (4 μm line width of type 3) to TSP was investigated. Figure 10 shows the operation of the touch sensor fabricated with the optimized mesh pattern. The touch sensor operated well, which indicates that the optimized mesh pattern is feasible in TSP applications.

4. CONCLUSION

In this study, the characteristics of a metal mesh touch sensor were enhanced by using an Mo/Al/Mo architecture metal mesh pattern. The thickness of the Mo/Al/Mo was optimized at 30/150/30 nm, and low sheet resistance below 0.27 Ω/□ was achieved with good adhesion on a glass substrate. Especially, thermal stability and corrosion resistance of the sheet resistance were enhanced by covering the Al with Mo. The change in resistance of the Mo/Al/Mo layer architecture was less than 0.056 even after heat-treatment at 260 °C. By using the optimized architecture, the mesh pattern with a 4 μm line width showed good optical transmittance (86.7%) and reflectivity (13.1%) at 550 nm, respectively. The touch sensor fabricated by using the Mo/Al/Mo mesh pattern operated well indicating that the mesh pattern is feasible in TSP applications.

Acknowledgments: This study was supported by the Korea Institute for the Advancement of Technology (KIAT) grant funded by the Korea government Ministry of Trade, Industry and Energy (No. A006100046).

References and Notes

1. J.-Y. Ruan, P. C.-P. Chao, and W.-D. Chen, *IEEE Sensors 2010 Conf. Book*, Waikoloa, USA **(2010)**, p. 309.
2. T.-H. Hwang, W.-H. Cui, I.-S. Yang, and O.-K. Kwon, *IEEE Trans. Cons. Elec.* 56, 1115 **(2010)**.
3. P. T. Krein and R. D. Meadows, *IEEE Trans. Ind. Appl.* 26, 529 **(1990)**.
4. J. Groep, P. Spinelli, and A. Polman, *Nano Lett.* 12, 3138 **(2012)**.
5. D.-K. Shin and J. Park, *Displays* 35, 141 **(2014)**.
6. J. Y. Lee, S. T. Connor, Y. Cui, and P. Peumans, *Nano Lett.* 8, 689 **(2008)**.
7. ASTM Designation: D 3359–97.
8. L. Assmann, J. C. Bernède, A. Drici, C. Amory, E. Halgand, and M. Morsli, *Appl. Surf. Sci.* 246, 159 **(2005)**.
9. X. Dai, A. Zhou, L. Feng, Y. Wang, J. Xu, and J. Li, *Thin Solid Films* 567, 64 **(2014)**.

10. M.-Z. Gao, R. Job, D.-S. Xue, and W. R. Fahrner, *Chin. Phys. Lett.* 25, 1380 **(2008)**.
11. M. V. Zeller and J. A. Kargol, *Appl. Surf. Sci.* 18, 63 **(1984)**.
12. R. K. Sharma, P. C. H. Chan, Z. Tang, G. Yan, I.-M. Hsing, and J. K. O. Sin, *Sensor. Actuat. B-Chem.* 81, 9 **(2001)**.
13. JEDEC STANDARD, JESD22-A103C (Revision of JESD22-A103-B) November **(2004)**.
14. D. W. Yun, H. S. Seo, J. H. Jun, J. M. Lee, and K. Y. Kim, *Int. J. Hydrogen Energy* 37, 10328 **(2012)**.
15. C. M. Abreu, M. J. Cristóbal, R. Figueroa, and G. Pena, *Corros. Sci.* 54, 143 **(2012)**.
16. Z. Luo, G. Qu, Y. Zhang, L. Cui, and A. Lu, *J. Non-Crys. Sol.* 378, 45 **(2013)**.
17. A. F. Dericioglu, A. R. Boccaccini, I. Dlouhy, and Y. Kagawa, *Mater. Trans.* 46, 996 **(2005)**.

Received: 31 August 2014. Accepted: 15 March 2015.